Thermally activated flow in models of amorphous solids

Marko Popović ⬤, Tom W. J. de Geus ⬤, Wencheng Ji ⬤, and Matthieu Wyart
Institute of Physics, École Polytechnique Fédérale de Lausanne (EPFL), CH-1015 Lausanne, Switzerland

Amorphous solids yield at a critical value Σ_c of the imposed stress Σ through a dynamical phase transition. While sharp in athermal systems, the presence of thermal fluctuations leads to the rounding of the transition and thermally activated flow even below Σ_c. Here we study the steady-state thermal flow of amorphous solids using a mesoscopic elastoplastic model. In the Hébraud-Lequex (HL) model we provide an analytical solution of the thermally activated flow at low temperature. We then propose a general scaling law that also describes the transition rounding. Finally, we find that the scaling law holds in numerical simulations of the HL model, a two-dimensional (2D) elastoplastic model, and previously published molecular dynamics simulations of 2D Lennard-Jones glass.

I. INTRODUCTION

Amorphous solids as diverse as metallic glasses, colloidal glasses, emulsions, foams, and granular matter exhibit a finite yield stress Σ_c beyond which they begin to flow. In athermal systems, this corresponds to a sharp yielding transition, separating solid and fluid phases, which has been extensively studied [1,2]. At finite temperature, the transition is rounded by thermally activated flow and becomes a smooth crossover. Understanding the properties of the thermally activated flow is a problem of both fundamental and practical importance.

Plastic deformation of amorphous solids proceeds through localized plastic events [3–5]. Each plastic event produces a localized nonaffine strain field which redistributes stresses in the material [6]. The ensuing dynamics has been described on a mesoscopic scale by shear transformation zone theory [4] and soft glassy rheology [7]. In these approaches, the mechanical noise produced by stress redistribution of individual events is described by an effective temperature. A different mesoscopic approach, the elastoplastic model, accounts for the stress redistribution induced by a local rearrangement [2,8]. In this model, yielding is a dynamical phase transition. The central quantity describing the system is the density $P(x)$ of regions about to undergo a plastic event, with x denoting the additional stress required locally to trigger an event. In the solid phase $P(x)$ is singular implying system spanning avalanches of plastic events [9,10], consistent with the observations in numerically simulated amorphous solids [11–13]. The flowing phase exhibits nonlinear rheology with a diverging correlation length as Σ_c is approached from above [14].

This phenomenology is similar to the one found in the depinning transition, where an elastic sheet is driven by a force density F through a disordered potential, and a critical value F_c separates moving and static states [15,16]. However, unlike for the yielding transition, stress redistribution after a depinning event is destabilizing everywhere, which leads to a nonsingular $P(x)$ and different exponents characterizing

the critical behavior close to the transition [10]. At finite temperature [17–24] a scaling law for the interface velocity $V \sim T^\psi g[(F - F_c)/T^{\psi/\beta}]$ was proposed by Fisher [17] in the context of charge density wave, where ψ is the transition rounding exponent and β is the athermal flow exponent $V \sim (F - F_c)^\beta$. It was further argued that $\psi = \beta/\alpha$ [18], where α is a parameter characterizing the disordered potential ($\alpha = 1.5$ for smooth potentials), which is supported by simulations [18,19]. On the other hand, numerical investigations of elastic string depinning [23,24] found a different value of the rounding exponent. Furthermore, in [25] the measured steady-state flow was found not to follow the scaling law from [17],[1] which was further supported by analysis of elastic line depinning in a washboard potential [26].

The thermal rounding of the yielding transition has been much less studied. In Ref. [27] it was proposed that the thermal fluctuations can be incorporated in the athermal steady-state flow $\dot{\gamma} \sim (\Sigma - \Sigma_c)^\beta$ as an additive, strain rate dependent, correction of local yield stresses. This approach, supported by molecular dynamics simulations, predicts an exponentially suppressed steady-state strain rate $\ln \dot{\gamma} \sim (\Sigma_c - \Sigma)^{3/2}/T$ for $\Sigma_c - \Sigma \gg T^{2/3}$. Here the exponent 3/2 is a particular value of α for a smooth disordered potential. In this regime, a gap is found in distribution $P(x)$, and the assumption of additivity corresponds to assuming that the gap size is proportional to $\Sigma_c - \Sigma$. In the regime $\Sigma - \Sigma_c \gg T^{2/3}$ flow is dominated by the athermal component and thus well described by construction. It is interesting to note that the rounding exponent at $\Sigma = \Sigma_c$ is consistent with the prediction of Ref. [18], up to a logarithmic correction. However, in this

---

[1]Instead, an alternative scaling law was proposed from which follows a logarithmic correction to the rounding exponent. However, the latter is derived by considering the limit $T \to 0$ in a finite system. It remains to be seen if this result holds when the thermodynamic limit is taken first.

approach, the influence of elastic interactions on the distribution $P(x)$ is not considered.

In this work, we study the thermal flow of amorphous solids for different values of the parameter α. In particular, we first study the thermal steady-state flow and $P(x)$ in a Hébraud-Lequeux (HL) model [28,29] which is a mean-field version of elastoplastic model with a Gaussian mechanical noise. (Note that here we do not consider the mean-field elastoplastic model [30], which preserves the fat tails in mechanical noise distribution found in a finite-dimensional elastoplastic model, where our scaling analysis should hold but for which we do not have analytical solutions.) We derive analytical expressions for both steady-state flow and $P(x)$ in the limit $T \to 0$ and verify these results numerically. We find that the strain rate in the HL model can be written in the scaling form as proposed by Fisher [17] and Middleton [18]. Finally, we propose that this scaling form holds in finite dimensions with a particular form of the scaling function in the regime $\Sigma_c - \Sigma \gg T^{1/\alpha}$ and test it in the HL model, a two-dimensional (2D) elastoplastic model, and molecular dynamics simulations available in the literature [27].

II. ELASTOPLASTIC MODEL AT FINITE TEMPERATURE

Elastoplastic models aim to capture mesoscopic features of yielding in amorphous solids [2,31,32]. The system is divided into N mesoscopic blocks that are larger than localized plastic events. A block i is characterized by the local stress component σ_i along the external loading direction and a local yield stress $\sigma_{Y,i}$. We choose $\sigma_{Y,i}$ to be narrowly distributed around the mean value $\langle \sigma_Y \rangle$ (see the Appendix).[2]

In athermal systems, the block i fails when $|\sigma_i| \geqslant \sigma_{Y,i}$. Then, over a time τ the local stress is decreased by an amount $\delta\sigma_i$, which in our numerical implementation is equal to σ_i up to a small random term; see the Appendix. It corresponds to an increment of local plastic strain of magnitude $\gamma_{0,i}$. In our implementation we choose $\gamma_{0,i} = \delta\sigma_i/\langle\sigma_Y\rangle$. The stress in the rest of the system is redistributed according to an elastic force dipole propagator $\delta\sigma_i G(\vec{r})$, where $\vec{r}$ is the distance from the failing block.

To study thermal plastic flow we introduce a possibility of thermal activation when $|\sigma_i| < \sigma_{Y,i}$. To each block we assign a potential barrier $E_i = c_E x_i^\alpha$, where $x_i \equiv (\sigma_{Y,i} - \sigma_i)/\langle\sigma_Y\rangle$ and $c_E > 0$. In a system with a smooth disorder potential a plastic event corresponds to saddle-node bifurcation and $\alpha = 1.5$. We also consider values $\alpha = 2$ and $\alpha = 1$ corresponding to parabolic and linear potentials with a cusp at the instability [25]. The failure probability for the block i with $x_i > 0$ is proportional to $\exp(-c_E x_i^\alpha/T)$, using units where $k_B = 1$. The imposed shear stress in the system sets the average block stress $\Sigma \equiv \sum_i \sigma_i/N = \langle\sigma_Y\rangle(1 - \sum_i x_i/N)$. The plastic strain rate is the sum of rates over individual plastic events $\dot\gamma \equiv \sum_i n_i \gamma_{0,i}/(\tau N)$, where $n_i = 1$ as long as the block is failing, while $n_i = 0$ otherwise. In the yielding regime $|\Sigma_c - \Sigma| \ll \Sigma_c$, at low strain rates blocks fail at $\sigma_i \approx \langle\sigma_Y\rangle$ and thus $\gamma_{0,i} \approx$

1, so that the plastic strain rate can be approximated by the rate of plastic events $\dot\gamma \approx \sum_i n_i/(\tau N)$.

Finally, to express this elastoplastic model in dimensionless quantities we use $\tilde{t} = t/\tau$, $\tilde{\Sigma} = \Sigma/\langle\sigma_Y\rangle$, $\dot{\tilde{\gamma}} = \dot\gamma\tau/\gamma_0$, $\tilde{T} = T/c_E$, where γ_0 is a typical value of $\gamma_{0,i}$. Here we normalized the temperature by the potential barrier energy scale c_E and the dimensionless parameter $\tilde{c}_E = c_E/(\gamma_0\langle\sigma_Y\rangle a^d)$, where d is the spatial dimension and a is the block size, characterizes a particular physical system.

III. FLOW IN HéBRAUD-LEQUEUX MODEL

A. Framework

We introduce an activated version of the Hébraud-Lequeux model where the state of the system is fully described by the density $P(x, \tilde{t})$ whose dynamics follows:

$$\partial_{\tilde{t}} P(x, \tilde{t}; \tilde{T}) = \dot{\tilde{\gamma}}\left[D\partial_x^2 P(x, \tilde{t}; \tilde{T}) + v\partial_x P(x, \tilde{t}; \tilde{T}) + \delta(x - 1)\right] - \left[\Theta(-x) + e^{-\frac{x^\alpha}{\tilde{T}}}\Theta(x)\right]P(x, \tilde{t}; \tilde{T}). \quad (1)$$

Here Θ is the Heaviside theta function, the diffusion constant D characterizes the Gaussian mechanical noise experienced by the system after each plastic event, the drift velocity v accounts for the externally controlled stress loading, and stress relaxation after a failure is described by the delta function term.[3] The last two terms account for athermal and thermally activated block failures, respectively. In a driven system it is very unlikely for a block to fail with $\sigma_i < -\sigma_Y$, and we neglect this contribution.[4]

The system stress is given by:

$$\tilde{\Sigma} = 1 - \int_{-\infty}^{\infty} x P(x, \tilde{t}; \tilde{T}) \, dx. \quad (2)$$

In this work we consider only steady-state flows, and the strain rate is equal to the plastic strain rate:

$$\dot{\tilde{\gamma}} = \int_{-\infty}^{\infty} P(x, \tilde{t}; \tilde{T})\left[\Theta(-x) + \Theta(x)e^{-\frac{x^\alpha}{\tilde{T}}}\right] dx. \quad (3)$$

B. Gap at $T = 0$

The full solution of Eq. (1) is in general not available. However, we can calculate the strain rate $\dot{\tilde{\gamma}}$ for $\tilde{\Sigma}_c - \tilde{\Sigma} \ll \tilde{\Sigma}_c$ and $\tilde{T}^{1/\alpha} \ll \tilde{\Sigma}_c - \tilde{\Sigma}$. Below $\tilde{\Sigma}_c$ there is no flow in the absence of temperature, and therefore plastic events mainly occur by thermal activation. Therefore, in the limit $\tilde{T} \to 0$, we expect an Arrhenius type of flow $\dot{\tilde{\gamma}} \sim \exp(-A/\tilde{T})$, with $A > 0$. Given this assumption we show that a gap appears in $P_0(x) \equiv \lim_{\tilde{T}\to 0} P(x)$ by considering the steady state of Eq. (1):

$$0 = D\partial_x^2 P(x) + v\partial_x P(x) + \delta(x - 1) - \frac{1}{\dot{\tilde{\gamma}}}\left[\Theta(-x) + e^{-\frac{x^\alpha}{\tilde{T}}}\Theta(x)\right]P(x). \quad (4)$$

---

[2]We expect this choice not to affect the universal properties studied here, as they should not change with the choice of microscopic parameters.

[3]This corresponds to $\delta\sigma_i = \sigma_i$ at each block failure, with the choice $\sigma_{Y,i} = 1$.

[4]For a block to reach $x = 2$ starting from $x = 1$ it has to diffuse distance $\Delta x = 1$ against the imposed stress. Common values [8] are $D = 0.18$ and $v \approx 1$ so only $\exp(-v/D) \approx 0.004$ of blocks that start from $x = 1$ reach $x = 2$.

In the limit $T \to 0$, for $x < A^{1/\alpha}$ the relative failure rate $\exp(-x^\alpha/\tilde{T})/\dot{\gamma}$ diverges, and for $x > A^{1/\alpha}$ it vanishes. Therefore, the point $x_c = A^{1/\alpha}$ acts as an absorbing boundary. For $x > x_c$, $P_0(x)$ satisfies:

$$0 = D\partial_x^2 P_0(x) + v_c \partial_x P_0(x) + \delta(x-1). \tag{5}$$

The solution of Eq. (5) is:

$$P_0(x) = \frac{1}{v_c}\left(1 - e^{-\frac{v_c}{D}(x-x_c)}\right)\Theta(x-x_c)\Theta(1-x)$$
$$+ \frac{1}{v_c}\left(1 - e^{-\frac{v_c(1-x_c)}{D}}\right)e^{-\frac{v_c}{D}(x-1)}\Theta(x-1). \tag{6}$$

Normalization of $P_0(x)$ requires $x_c = 1 - v_c$, and thus we can express the gap size x_c in terms of the stress $\tilde{\Sigma}$ by evaluating Eq. (2) in the limit $\tilde{T} \to 0$:

$$\tilde{\Sigma} = 1 - \int_{-\infty}^{\infty} x P_0(x)\, dx = \frac{1}{2}v_c - \frac{D}{v_c}, \tag{7}$$

and we find:

$$x_c = 1 - \tilde{\Sigma} - \sqrt{\tilde{\Sigma}^2 + 2D}. \tag{8}$$

Since $x_c \to 0$ as $\tilde{\Sigma} \to \tilde{\Sigma}_c$ we have $\tilde{\Sigma}_c = 1/2 - D$ so that for $(\tilde{\Sigma}_c - \tilde{\Sigma}) \ll \tilde{\Sigma}_c$:

$$x_c \simeq \frac{\tilde{\Sigma}_c - \tilde{\Sigma}}{\frac{1}{2} + D}. \tag{9}$$

C. Thermal rounding of $P(x)$

At a small but finite temperature the activation occurs in a region around x_c of a width vanishing with T. To find an approximation of $P(x)$ we linearize the potential barrier $E(x)$ around x_c and look for a solution of

$$D\partial_x^2 P(x) + v\partial_x P(x) - \frac{1}{\dot{\gamma}}e^{-\frac{x_c^\alpha}{\tilde{T}}}e^{-\frac{\alpha x_c^{\alpha-1}}{\tilde{T}}(x-x_c)}P(x) = 0. \tag{10}$$

Using a change of variables and functions

$$\tilde{R}(x) = e^{\frac{v}{2D}(x-x_c)}P(x), \tag{11}$$

$$z = \frac{2}{m}e^{-\frac{a}{2}(x-x_c)}, \tag{12}$$

$$R(z) = \tilde{R}(x), \tag{13}$$

we can rewrite Eq. (10) as

$$z^2 \partial_z^2 R(z) + z\partial_z R(z) - \left[\left(\frac{v}{aD}\right)^2 + z^2\right]R(z) = 0, \tag{14}$$

where

$$a \equiv \alpha\frac{x_c^{\alpha-1}}{\tilde{T}}, \tag{15}$$

$$m^2 \equiv a^2 D\dot{\gamma}e^{\frac{x_c^\alpha}{\tilde{T}}}. \tag{16}$$

Equation (14) is the modified Bessel equation, and the solution, which vanishes for $x \to -\infty$, reads

$$P(x) = Ce^{-\frac{v}{2D}(x-x_c)}K_{\frac{v}{aD}}\left(\frac{2e^{-\frac{a}{2}(x-x_c)}}{m}\right), \tag{17}$$

where $K_\lambda(x)$ is the modified Bessel function of the second kind, of order λ. Finally, we can determine the integration constant C and parameter m by requiring that $P(x) \to P_0(x)$ as $\tilde{T} \to 0$. In the limit $\tilde{T} \to 0$ and for $x > x_c + \epsilon, \epsilon > 0$, the lowest order terms in the series representation of the Bessel function are:

$$K_{\frac{v}{aD}}\left(\frac{2e^{-\frac{a}{2}(x-x_c)}}{m}\right) \approx \frac{1}{2}\Gamma\left(\frac{v}{aD}\right)m^{\frac{v}{aD}}e^{\frac{v}{2D}(x-x_c)}$$
$$+ \frac{1}{2}\Gamma\left(-\frac{v}{aD}\right)m^{-\frac{v}{aD}}e^{-\frac{v}{2D}(x-x_c)}, \tag{18}$$

where Γ is the gamma function. We assume that $\dot{\gamma}\exp(x_c^\alpha/\tilde{T})$ does not depend exponentially on $\tilde{T}$ so that higher order terms are negligible when $\tilde{T} \to 0$. Equating $P(x)$ with $P_0(x)$ in the limit $\tilde{T} \to 0$ yields

$$C = \frac{2m^{-\frac{v}{aD}}}{v_c\Gamma\left(\frac{v}{aD}\right)}, \tag{19}$$

$$m = e^{\overline{\gamma}}, \tag{20}$$

where $\overline{\gamma}$ is the Euler-Mascheroni constant. With these expressions Eq. (17) provides a solution of $P(x)$ in the vicinity of x_c.

Finally, from Eq. (16) and Eq. (20), the thermal flow in the low-temperature limit $\tilde{T}^{1/\alpha} \ll \tilde{\Sigma}_c - \tilde{\Sigma}$ is

$$\dot{\gamma} = \frac{e^{2\overline{\gamma}}}{\alpha^2 D\tau}\tilde{T}^2\left(\frac{\tilde{\Sigma}_c - \tilde{\Sigma}}{\frac{1}{2} + D}\right)^{-2(\alpha-1)}e^{-\frac{1}{(\frac{1}{2}+D)^\alpha}\frac{(\tilde{\Sigma}_c-\tilde{\Sigma})^\alpha}{\tilde{T}}}. \tag{21}$$

The thermal flow is exponentially small in $(\tilde{\Sigma}_c - \tilde{\Sigma})^\alpha$, consistent with [27,33]. It can be written in scaling form

$$\dot{\gamma} \sim T^{\frac{2}{\alpha}}f_{HL}\left(\frac{\Delta\tilde{\Sigma}}{\tilde{T}^{1/\alpha}}\right), \tag{22}$$

where $\Delta\tilde{\Sigma} \equiv \tilde{\Sigma} - \tilde{\Sigma}_c$ and $\lim_{y \to -\infty} f_{HL}(y) = |y|^{2(1-\alpha)}\exp(-c|y|^\alpha)$ with $c = 1/(1/2+D)^\alpha$. Since the flow exponent $\beta = 2$ in the HL model this scaling form is consistent with the prediction $\psi = \beta/\alpha$ in [18].

IV. SCALING LAW

We propose the scaling form in Eq. (22) to hold in finite-dimensional systems as

$$\dot{\gamma} \sim \tilde{T}^\psi f\left(\frac{\Delta\tilde{\Sigma}}{\tilde{T}^{1/\alpha}}\right), \tag{23}$$

where $\psi = \beta/\alpha$ and β is the athermal flow exponent $\dot{\gamma} \sim \Delta\tilde{\Sigma}^\beta$. This form is the same as the one suggested by Fisher for thermal flow in depinning [17]. This scaling hypothesis assumes a characteristic stress scale $|\Delta\tilde{\Sigma}| \sim T^{1/\alpha}$, set by the activation $e^{-x^\alpha/\tilde{T}}$ in the vicinity of the transition. The thermal rounding exponent $\psi = \beta/\alpha$ then follows by considering the athermal limit $\tilde{T}^{1/\alpha} \ll \Delta\tilde{\Sigma}$ in the vicinity of the transition. In this limit we conclude that $\lim_{y \to \infty} f(y) \sim y^\beta$, and therefore $\psi = \beta/\alpha$, in order to match the athermal flow.

Moreover, to propose the form of the scaling function f in the thermally activated flow regime $\tilde{\Sigma}_c - \tilde{\Sigma} \gg \tilde{T}^{1/\alpha}$ we consider a system in the limit $\tilde{T} \to 0$ with a finite gap x_c. In this limit blocks become unstable in the vicinity of x_c, and the potential barrier in the activation function can be expanded to the first order around the gap x_c as in

Eq. (10): $\exp\left(-x_c^\alpha/\tilde{T}\right)\exp\left[-\alpha x_c^{\alpha-1}(x-x_c)/\tilde{T}\right]$. The first factor can be interpreted as a new timescale $\tilde{\tau}(x_c) = \exp\left(x_c^\alpha/\tilde{T}\right)$, and the second factor as a new effective activation function $\exp\left[-(x-x_c)^{\alpha_{\text{eff.}}}/\tilde{T}_{\text{eff.}}\right]$, with effective values $\alpha_{\text{eff.}} = 1$ and $\tilde{T}_{\text{eff.}} = \tilde{T}/(\alpha x_c^{\alpha-1})$.

Since in the limit $\tilde{T}\to 0$ the effective absorbing boundary is at x_c, we expect that in the vicinity of x_c the distribution $P_0(x) = \lim_{\tilde{T}\to 0} P(x)$ corresponds to an athermal $P(x)$ of a system at a critical stress. Therefore, in this state the system will respond to adding a small amount of temperature in the same way as a system at the critical stress. The flow can thus be described by the thermal rounding exponent $\dot{\gamma}\sim \tilde{T}_{\text{eff.}}^{\beta/\alpha_{\text{eff.}}}/\tilde{\tau}(x_c)$ leading to:

$$\dot{\gamma} \sim x_c^{-\beta(\alpha-1)}\tilde{T}^\beta e^{-\frac{x_c^\alpha}{\tilde{T}}} \tag{24}$$

$$\sim |\Delta\tilde{\Sigma}|^{-\beta(\alpha-1)}\tilde{T}^\beta e^{-c\frac{|\Delta\tilde{\Sigma}|^\alpha}{\tilde{T}}}. \tag{25}$$

The last relation stems from $x_c \sim |\Delta\tilde{\Sigma}|$, i.e., the existence of a unique vanishing stress scale at $\tilde{\Sigma}_c$, and c is a positive parameter. Therefore, the scaling function in the thermally activated regime reads:

$$f(y\ll -1) \sim |y|^{\beta(1-\alpha)}e^{-c|y|^\alpha}. \tag{26}$$

V. NUMERICAL TESTS

To test the analytical results obtained in the HL model and the proposed finite-dimensional scaling form for $\dot{\gamma}$ we perform numerical simulations using HL and 2D elastoplastic models; see the Appendix for details.

A. Hébraud-Lequeux model

We first compare the analytical approximation of the density $P(x)$ in the vicinity of x_c in Eq. (17) to the one obtained in HL model simulations. We find a good agreement between simulations and the analytical result for $\alpha = 1$ at all tested temperatures; see Fig. 1(a). For $\alpha = 1.5$ the analytical approximation fails at higher temperatures, but a good agreement is recovered at lower temperatures; see Fig 1(b). This is expected since the analytical solution was obtained assuming $\tilde{T}^{1/\alpha}\ll x_c$, which does not hold at higher temperatures, and consequently the linearization of x^α is not justified.

We next compare the analytical prediction in Eq. (21) and the proposed general scaling form Eq. (23) with the results of HL and 2D elastoplastic model simulations for $\alpha = 1, 1.5, 2$. We find that the strain rate measured at different temperatures collapses when the axes are scaled according to the proposed scaling form; see Fig. 2. The analytical prediction of the mean-field strain rate given by Eq. (21) is shown as a black line in Fig. 2, and it is in good agreement with numerical simulations at low temperatures in the thermally activated regime $\tilde{\Sigma}_c - \tilde{\Sigma}\gg\tilde{T}^{1/\alpha}$.

B. 2D elastoplastic model

We further test the generalized scaling form in Eq. (23) using elastoplastic simulations in two dimensions for $\alpha = 1, 1.5, 2$. The flow exponent measured in [30] for this
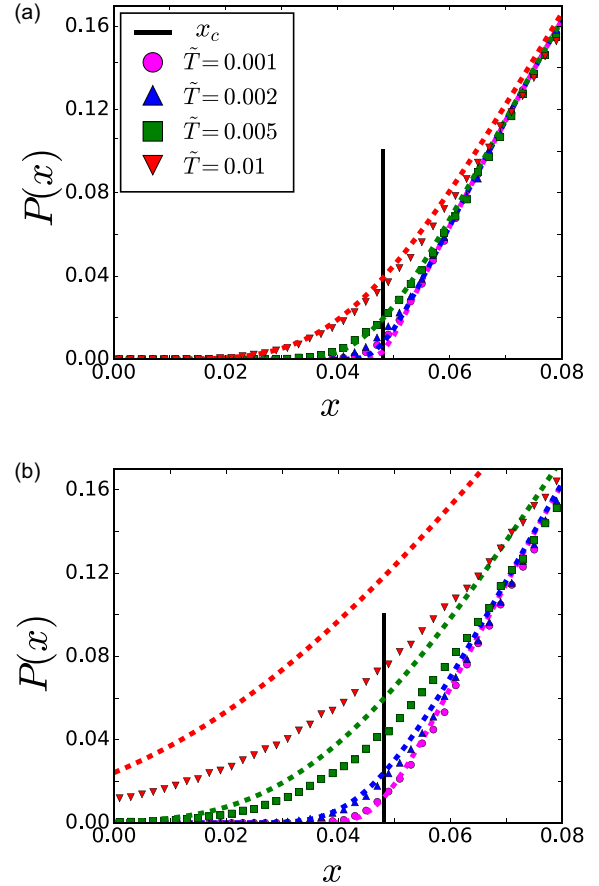

FIG. 1. Distribution $P(x)$ measured in HL model simulations (symbols) compared to the analytical approximation Eq. (17) (dashed lines) in the vicinity of the gap x_c, indicated by a black line. (a) For $\alpha = 1$ simulations and theory agree well at all measured temperatures. (b) For $\alpha = 1.5$ the agreement is good at the lowest measured temperatures, but it becomes significantly poorer at higher temperatures, as expected since the linearization of thermal activation function is not a valid approximation.

model is $\beta = 1.52$. We find that the steady-state flow rate collapses on a single curve when axes are scaled according to Eq. (23); see Fig. 3. We demonstrate that increasing system size from $N = 20\,164$ (full symbols) to $N = 99\,856$ (empty symbols) does not affect the scaling function. Furthermore, the scaling function Eq. (26), represented by a black dashed line, is consistent with simulation data for all three values of α.

C. Molecular dynamics

Finally, to further verify the generality of the proposed scaling law, we extract strain rate curves obtained by molecular dynamics simulations of 2D glass in Ref. [27]. The good collapse of data when the axes are scaled according to Eq. (23) is shown in Fig. 4. The scaling function we propose in Eq. (26), shown as dashed black line, is consistent with the data. Note that we normalized stress and temperature by shear elastic modulus and potential barrier scale using the values provided in [27].
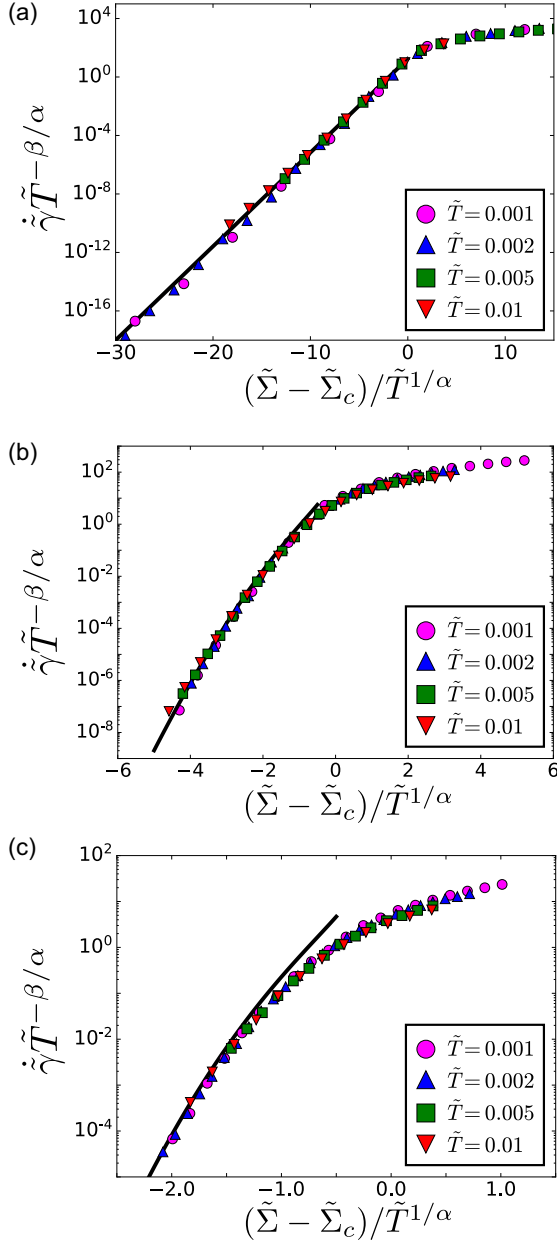
FIG. 2. Strain rate measured in numerical simulations using the HL model, using the values $\alpha = 1$ (a), $\alpha = 3/2$ (b), and $\alpha = 2$ (c). The flow exponent in the HL model is $\beta = 2$ [28]. When scaled according to the proposed scaling law Eq. (23), the strain rates collapse. System size is $N = 20\,000$. In addition, we find the analytical solution Eq. (21) (black solid line) is in excellent agreement with the simulations in the regime $\tilde{T}^{1/\alpha} \ll \tilde{\Sigma}_c - \tilde{\Sigma}$ for which the solution was derived.
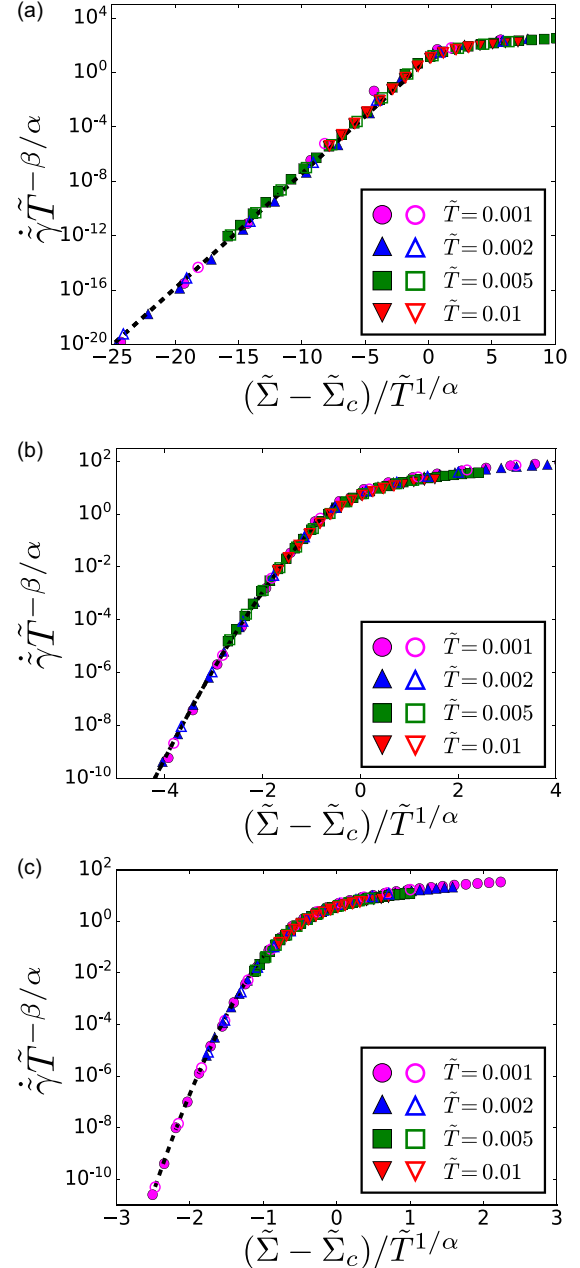
FIG. 3. Strain rate measured in numerical simulations using the 2D elastoplastic model, using the values $\alpha = 1$ (a), $\alpha = 3/2$ (b), and $\alpha = 2$ (c). The flow exponent for this model is $\beta = 1.52$ [30]. When scaled according to the proposed scaling law Eq. (23), the strain rates collapse. To test finite-size scaling we show results obtained in system sizes $N = 20\,164$ (full symbols) and $N = 99\,856$ (empty symbols). The proposed scaling function in Eq. (26), shown with the dashed black line, can account for the thermally activated regime.

VI. DISCUSSION

We have derived an approximation of thermally activated steady-state strain rate in HL model of amorphous solids. We confirmed the validity of this expression with numerical simulations and generalized this result to a general scaling law for the steady-state strain rate. We find that the proposed scaling form collapses both strain rate data from a 2D elastoplastic model and from molecular dynamics simulations [27]. Our

results support that the thermally activated flow of amorphous solids can be described by a simple scaling law dependent only on the flow exponent β and a parameter α reflecting properties of the disordered potential.

It is interesting to note that values of α different from 1.5 have practical applications, for example, in cellular materials such as epithelial tissues or dry foams $\alpha = 2$ [34]. While thermal fluctuations are usually negligible in foams,
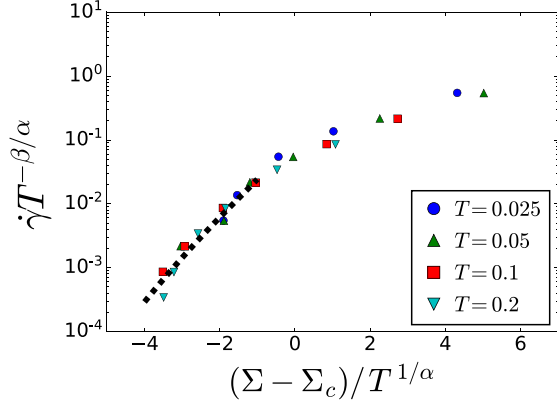
FIG. 4. Steady-state strain rate measured in molecular dynamics simulations of 2D glass extracted from [27]. We replotted the strain rate data as a function of $\Sigma - \Sigma_c$ on axes scaled according to the proposed scaling law Eq. (23). In this model particle interactions are smooth ($\alpha = 1.5$), and the flow exponent was measured to be $\beta = 2$. We find a good collapse of the data, indicating that Eq. (23) holds beyond elastoplasic models. To have comparable values of control parameter $(\Sigma - \Sigma_c)/T^{1/\alpha}$ with Figs. 2 and 3, stress and temperature are normalized by shear modulus κ and potential barrier scale c_E, respectively, using the reported values [27]. The proposed scaling function in Eq. (26) is shown as the dashed black line.

mechanical noise from active processes in tissues can be a relevant factor in tissue flow [35,36], and future research of yield stress behavior in biological tissues will be able to utilize and test results presented here.

The scaling form of the steady-state strain rate was originally proposed in the context of depinning, and it seems to describe well the rounding of the yielding transition in amorphous solids. The similarity between the two transitions is therefore useful to motivate further research of the yielding transition. An interesting research direction will be to study the low-stress regime $\tilde{\Sigma} \ll \tilde{\Sigma}_c$. In the corresponding depinning regime of low forcing $F \ll F_c$, the interface velocity grows with $\ln V \sim -F^{-\mu}$. The exponent μ is associated with a diverging length scale on which the interface has to reorganize to cross the effective potential barrier [37–39].

Finally, in this work, we have studied the steady-state flow where all information about the initial state of the material has been erased. Interestingly, amorphous solids can exhibit a complex transient flow characterized by an initial slowing, followed either by eventual arrest or by sudden fluidization. This phenomenon has been studied in the athermal HL and elastoplastic models [40,41]. However, it is important to understand the transient flow of thermal materials, where the arrest scenario is not available, and previously sharp transitions are smoothed on the stress scale $\Delta \tilde{\Sigma} \sim \tilde{T}^{1/\alpha}$.

APPENDIX: HEBRAUX-LEQUEUX AND ELASTOPLASTIC MODEL SIMULATIONS

1. Implementation

We implement the 2D elastoplastic model on a periodic lattice of linear size $L/a = 142$,[5] following the implementation we used in [42]. The elastic dipole propagator $G(r, \phi)$ is a periodic version of an infinite system propagator $G_0(r, \phi) \sim \cos 4\phi/r^2$, and it is normalized so that $G(\vec{r} = 0) = -1$. The sum of stresses along each row and column of elements is preserved. To keep the sum of stresses in all rows and columns the same during the initialization of the stress distribution $P(\tilde{\sigma})$ we first apply the dipole propagator with a random prefactor drawn from a normal distribution $\mathcal{N}(0, 0.4^2)$ at each lattice block and then normalize the stress at each block by the sum of the absolute values of the propagator on the periodic lattice. The initial yield stress distribution $P(\tilde{\sigma}_Y)$ is a normal distribution $\mathcal{N}(1, 0.1^2)$ and redrawn each time the block fails. These choices ensure that no stress overshoot and no shear banding occurs during the transient loading period.

After a failure local stress in the block is drawn from a normal distribution $\tilde{\sigma}_{i,\text{after}} = \mathcal{N}(0, 0.1^2)$, which defines the stress change in the block $\delta\tilde{\sigma}_i$.

The HL model simulations, in which blocks have no spatial information, contain $N = 20\,000$ blocks for the strain rate measurement and $N = 50\,000$ blocks for the $P(x)$ measurement. After each plastic event the stress is changed in all other blocks by an amount drawn independently from a normal distribution $\mathcal{N}(0, 2D/N)$, with $D = 0.18$.

To simulate thermal activation after each failure we draw the time until the next failure in the system from a Poisson distribution that takes into account all x in the system. Then we draw randomly the failing block by weighting each block with its failure rate $\exp(-x^\alpha/\tilde{T})$. In this way duration of a simulation is proportional to the plastic strain, independent of the strain rate.

2. Data analysis

To measure the steady-state strain rate $\dot{\tilde{\gamma}}$ and the distributions $P(x)$ we begin recording the state of the system only after it undergoes a plastic strain of 5. The steady-state strain rate is then measured by sampling the strain rate after every n_s plastic events up to the system plastic strain of 15 and then calculating the median.[6] In the HL model simulations $n_s = 100$ in all cases except $\alpha = 1, \tilde{T} = 0.001$, which required $n_s = 10$. In the 2D elastoplastic model simulations for system size $N = 20\,164$, $n_s = 1000$ in all cases except $\alpha = 1, \tilde{T} = 0.001$, which required $n_s = 100$, whereas for system size $N = 99\,856$ $n_s = 10$. The steady-state distribution $P(x)$ is measured in a system of size $N = 50\,000$ at the imposed stress $\tilde{\Sigma} = 0.29$ for the values of α and $\tilde{T}$ reported in Fig. 1.

Values of $\tilde{\Sigma}_c$ in the 2D elastoplastic model and HL model were estimated by collapsing the strain rate data in Figs. 2

---

[5]System size is $N = L^2$ and lattice size is $a = 1$.

[6]Note that at low temperatures sampling the strain rate over too large intervals becomes very susceptible to finite-size effects due to the exponential dependence of activation time on x

and 3. Note that this was also required in the HL model since the relation $\tilde{\Sigma}_c = 1/2 - D$ holds only in the thermodynamic limit, while in finite systems the value of $\tilde{\Sigma}_c$ is slightly modified by finite-size effects [14]. We find in the HL model $\Sigma_c = 0.323 \pm 0.002$ and in the 2D model $\Sigma_c = 0.5293 \pm 0.0007$.

[1] D. Bonn, M. M. Denn, L. Berthier, T. Divoux, and S. Manneville, Rev. Mod. Phys. **89**, 035005 (2017).

[2] A. Nicolas, E. E. Ferrero, K. Martens, and J.-L. Barrat, Rev. Mod. Phys. **90**, 045006 (2018).

[3] A. Argon, Acta Metall. **27**, 47 (1979).

[4] M. L. Falk and J. S. Langer, Phys. Rev. E **57**, 7192 (1998).

[5] P. Schall, D. A. Weitz, and F. Spaepen, Science **318**, 1895 (2007).

[6] C. E. Maloney and A. Lemaître, Phys. Rev. E **74**, 016118 (2006).

[7] P. Sollich, F. Lequeux, P. Hébraud, and M. E. Cates, Phys. Rev. Lett. **78**, 2020 (1997).

[8] J. Lin, A. Saade, E. Lerner, A. Rosso, and M. Wyart, Europhys. Lett. **105**, 26003 (2014).

[9] M. Müller and M. Wyart, Annu. Rev. Condens. Matter Phys. **6**, 177 (2015).

[10] J. Lin, T. Gueudré, A. Rosso, and M. Wyart, Phys. Rev. Lett. **115**, 168001 (2015).

[11] A. Lemaitre and C. Caroli, Phys. Rev. Lett. **103**, 065501 (2009).

[12] C. E. Maloney and M. O. Robbins, Phys. Rev. Lett. **102**, 225502 (2009).

[13] S. Karmakar, E. Lerner, I. Procaccia, and J. Zylberg, Phys. Rev. E **82**, 031301 (2010).

[14] J. Lin, E. Lerner, A. Rosso, and M. Wyart, Proc. Natl. Acad. Sci. USA **111**, 14382 (2014).

[15] D. S. Fisher, Phys. Rep. **301**, 113 (1998).

[16] T. Giamarchi, A. Kolton, and A. Rosso, in *Jamming, Yielding, and Irreversible Deformation in Condensed Matter*, Lecture Notes in Physics Vol. 688, edited by M. Miguel and M. Rubi (Springer, Berlin, Heidelberg, 2006).

[17] D. S. Fisher, Phys. Rev. B **31**, 1396 (1985).

[18] A. A. Middleton, Phys. Rev. B **45**, 9465 (1992).

[19] L.-W. Chen and M. C. Marchetti, Phys. Rev. B **51**, 6296 (1995).

[20] U. Nowak and K. D. Usadel, Europhys. Lett. **44**, 634 (1998).

[21] L. Roters, A. Hucht, S. Lübeck, U. Nowak, and K. D. Usadel, Phys. Rev. E **60**, 5202 (1999).

[22] D. Vandembroucq, R. Skoe, and S. Roux, Phys. Rev. E **70**, 051101 (2004).

[23] S. Bustingorry, A. B. Kolton, and T. Giamarchi, Europhys. Lett. **81**, 26005 (2008).

[24] S. Bustingorry, A. B. Kolton, and T. Giamarchi, Phys. Rev. E **85**, 021144 (2012).

[25] V. H. Purrello, J. L. Iguain, A. B. Kolton, and E. A. Jagla, Phys. Rev. E **96**, 022112 (2017).

[26] A. B. Kolton and E. A. Jagla, Phys. Rev. E **102**, 052120 (2020).

[27] J. Chattoraj, C. Caroli, and A. Lemaitre, Phys. Rev. Lett. **105**, 266001 (2010).

[28] P. Hébraud and F. Lequeux, Phys. Rev. Lett. **81**, 2934 (1998).

[29] E. Agoritsas and K. Martens, Soft Matter **13**, 4653 (2017).

[30] J. Lin and M. Wyart, Phys. Rev. X **6**, 011005 (2016).

[31] J.-C. Baret, D. Vandembroucq, and S. Roux, Phys. Rev. Lett. **89**, 195506 (2002).

[32] G. Picard, A. Ajdari, F. Lequeux, and L. Bocquet, Phys. Rev. E **71**, 010501(R) (2005).

[33] W. L. Johnson and K. Samwer, Phys. Rev. Lett. **95**, 195501 (2005).

[34] M. Popović, V. Druelle, N. A. Dye, F. Jülicher, and M. Wyart, New J. Phys. **23**, 033004 (2021).

[35] D. Bi, X. Yang, M. C. Marchetti, and M. L. Manning, Phys. Rev. X **6**, 021011 (2016).

[36] D. A. Matoz-Fernandez, E. Agoritsas, J.-L. Barrat, E. Bertin, and K. Martens, Phys. Rev. Lett. **118**, 158105 (2017).

[37] T. Nattermann, Europhys. Lett. **4**, 1241 (1987).

[38] P. Chauve, T. Giamarchi, and P. Le Doussal, Phys. Rev. B **62**, 6241 (2000).

[39] E. E. Ferrero, L. Foini, T. Giamarchi, A. B. Kolton, and A. Rosso, Phys. Rev. Lett. **118**, 147208 (2017).

[40] C. Liu, K. Martens, and J.-L. Barrat, Phys. Rev. Lett. **120**, 028004 (2018).

[41] C. Liu, E. E. Ferrero, K. Martens, and J.-L. Barrat, Soft Matter **14**, 8306 (2018).

[42] M. Popović, T. W. J. de Geus, and M. Wyart, Phys. Rev. E **98**, 040901(R) (2018).